

Anderson impurity in pseudo-gap Fermi systems

R. Bulla¹, Th. Pruschke² and A. C. Hewson¹

¹*Department of Mathematics, Imperial College,
180 Queen's Gate, London SW7 2BZ, United Kingdom*

²*Institut für Theoretische Physik der Universität,
93040 Regensburg, Germany*

(October 6, 2018)

We use the numerical renormalization group method to study an Anderson impurity in a conduction band with the density of states varying as $\rho(\omega) \propto |\omega|^r$ with $r > 0$. We find two different fixed points: a local-moment fixed point with the impurity effectively decoupled from the band and a strong-coupling fixed point with a partially screened impurity spin. The specific heat and the spin-susceptibility show powerlaw behaviour with different exponents in strong-coupling and local-moment regime. We also calculate the impurity spectral function which diverges (vanishes) with $|\omega|^{-r}$ ($|\omega|^r$) in the strong-coupling (local moment) regime.

PACS 75.20.Hr

I. INTRODUCTION

The behaviour of a magnetic impurities in metals is one of the best studied problem in condensed matter theory [1]. In most cases it is a very good approximation to replace the conduction density of states by a constant as small variations of the density of states do not lead to a qualitative change of the physical properties (like the complete screening of the impurity spin by the conduction electrons).

The question, whether these physical properties are different when the impurity is coupled to a Fermi system with a power-law density of states $\rho(\omega) \propto |\omega|^r$ near the Fermi-level was first discussed by Withoff and Fradkin [2].

A number of systems are expected to show this pseudo-gap density of states. Among these are certain heavy-fermion superconductors [3] where the exponent r can take the values $r = 1$ or $r = 2$ depending on the symmetry of the gap function. Other candidates are semiconductors whose valence and conduction bands touch at the Fermi level [4]. In quasi one-dimensional metals, which can be viewed as realizations of the Luttinger model, the exponent r is a function of the Coulomb interaction [5] and can take values between $r \ll 1$ and $r > 1$.

Recently, the numerical renormalization group method (NRG) [6,7] has been applied by Chen and Jayaprakash [8] (referred to as CY) and Ingersent [9] to the model of an impurity spin coupled to a conduction band with a power-law density of states. In principal, this Kondo model can be related to a corresponding Anderson model in the limit of $J \rightarrow 0$ via a standard Schrieffer-Wolff transformation [10]. There is, however, a transition between a strong-coupling (SC) fixed point and a local-moment (LM) fixed point for the Kondo model at *finite* J so that it is a priori not clear whether the behaviour at this transition will be the same in the Anderson version of the model.

The results of CY and Ingersent can be summarized

as follows. For any $J > J_c$ the system approaches some kind of SC fixed point with the difference to the standard Kondo model ($r = 0$) that the impurity spin is not completely screened (a residual magnetic moment of $r/8$ always remains in the zero-temperature limit). This can be qualitatively understood from the gradually decreasing density of states of the conduction electrons at the Fermi level which are responsible for the screening.

The thermodynamic quantities show non-Fermi liquid behaviour in the SC regime

$$\gamma(T) = \frac{C(T)}{T} \propto T^{-r}, \quad (1)$$

$$\chi_S(T) = \frac{r}{8}T^{-1} + aT^{-r} + bT^{-2r}, \quad (2)$$

(with $a, b = \text{const.}$). The critical line $J_c(r)$ starts linearly for small r but diverges at $r = \frac{1}{2}$. In addition, Ingersent has shown that this divergence only holds in the particle-hole symmetric case and that a finite J_c is restored away from this symmetry. (This reduction of J_c has implications for the observability of the crossover in experimental situations.)

For any $J < J_c$, the system approaches the LM fixed point where the impurity is effectively decoupled from the conduction band and a residual magnetic moment of $1/4$ remains. The thermodynamics in this regime have not yet been investigated.

In this paper, we want to study the behaviour of an Anderson impurity in a pseudo-gap fermion system where we restrict ourselves to the symmetric case. In Sec. II, we want to describe our approach to the generalization of the NRG with a non-constant density of states, and outline the differences to that of CY and Ingersent. The resulting formula for the hopping matrix elements of the semi-infinite chain for *all* n is given in Sec. III. The numerical results for static properties and the spectral function are discussed in Sec. IV and V, respectively.

II. GENERALIZATION OF NRG TO NONCONSTANT DENSITY OF STATES

The Hamiltonian we want to study in this paper is the conventional single-impurity Anderson model

$$H = \sum_{\sigma} \varepsilon_f f_{-1\sigma}^{\dagger} f_{-1\sigma} + U f_{-1\uparrow}^{\dagger} f_{-1\uparrow} f_{-1\downarrow}^{\dagger} f_{-1\downarrow} + \sum_{k\sigma} \varepsilon_k c_{k\sigma}^{\dagger} c_{k\sigma} + \sum_{k\sigma} V(\varepsilon_k) \left(f_{-1\sigma}^{\dagger} c_{k\sigma} + c_{k\sigma}^{\dagger} f_{-1\sigma} \right). \quad (3)$$

In the model (3), $c_{k\sigma}^{(\dagger)}$ denote standard annihilation (creation) operators for band states with spin σ and energy ε_k , $f_{-1,\sigma}^{(\dagger)}$ those for impurity states with spin σ and energy ε_f . The Coulomb interaction for two electrons at the impurity site is given by U and both subsystems are coupled via an energy dependent hybridization $V(\varepsilon_k)$ [11].

In the following we show that the Hamiltonian (3) is equivalent to a form which is more convenient for the derivation of the NRG equations

$$H = \sum_{\sigma} \varepsilon_f f_{-1\sigma}^{\dagger} f_{-1\sigma} + U f_{-1\uparrow}^{\dagger} f_{-1\uparrow} f_{-1\downarrow}^{\dagger} f_{-1\downarrow} + \sum_{\sigma} \int_{-1}^1 d\varepsilon g(\varepsilon) a_{\varepsilon\sigma}^{\dagger} a_{\varepsilon\sigma} + \sum_{\sigma} \int_{-1}^1 d\varepsilon h(\varepsilon) \left(f_{-1\sigma}^{\dagger} a_{\varepsilon\sigma} + a_{\varepsilon\sigma}^{\dagger} f_{-1\sigma} \right), \quad (4)$$

where we introduced a one-dimensional energy representation for the conduction band with band cut-offs at ± 1 , dispersion $g(\varepsilon)$ and hybridization $h(\varepsilon)$. The band operators fulfil the standard fermionic commutation rules $[a_{\varepsilon\sigma}^{\dagger}, a_{\varepsilon'\sigma'}] = \delta(\varepsilon - \varepsilon') \delta_{\sigma\sigma'}$.

To establish the equivalence of the Hamiltonians (3) and (4) we prove that for a specific choice of $g(\varepsilon)$ and $h(\varepsilon)$ they lead to the same effective action for the impurity degree of freedom. This effective action is obtained by integrating over the conduction electron degrees of freedom. For the Hamiltonian (3) one gets

$$S_{\text{eff}}(\psi, \psi^{\dagger}) = S_f(\psi, \psi^{\dagger}) + \left(\frac{\beta}{N} \right)^2 \sum_{\sigma n m} \psi_{\sigma n+1}^{\dagger} \psi_{\sigma m-1} \sum_k V(\varepsilon_k)^2 G_{nm}^c(k), \quad (5)$$

(see for example [12]). n and m count the steps on the imaginary time axis $[0, \beta]$ with N the number of steps. ψ and ψ^{\dagger} are Grassmann numbers corresponding to the impurity operators. S_f describes the unhybridized impurity. The $G_{nm}^c(k)$ are Green functions for the free conduction electron system.

The action corresponding to the Hamiltonian (4) can be written as

$$S(\psi, \psi^{\dagger}, \chi, \chi^{\dagger}) = S_f(\psi, \psi^{\dagger})$$

$$+ \sum_{\sigma n} \int_{-1}^1 d\varepsilon \chi_{\varepsilon\sigma n}^{\dagger} \left(\left(1 - \frac{\beta}{N} g(\varepsilon) \right) \chi_{\varepsilon\sigma n-1} - \chi_{\varepsilon\sigma n} \right) - \frac{\beta}{N} \sum_{\sigma n} \int_{-1}^1 d\varepsilon h(\varepsilon) \left[\chi_{\varepsilon\sigma n}^{\dagger} \psi_{\sigma n-1} + \psi_{\sigma n}^{\dagger} \chi_{\varepsilon\sigma n-1} \right]. \quad (6)$$

$\chi_{\varepsilon\sigma n}^{\dagger}$ and $\chi_{\varepsilon\sigma n}$ are Grassmann numbers corresponding to the conduction electron operators $a_{\varepsilon\sigma}^{\dagger}$ and $a_{\varepsilon\sigma}$. Integrating over the conduction electron degrees of freedom leads to

$$S_{\text{eff}}(\psi, \psi^{\dagger}) = S_f(\psi, \psi^{\dagger}) + \left(\frac{\beta}{N} \right)^2 \sum_{\sigma n m} \psi_{\sigma n+1}^{\dagger} \psi_{\sigma m-1} \int_{-1}^1 d\varepsilon h(\varepsilon)^2 G_{nm}^c(g(\varepsilon)). \quad (7)$$

To compare the effective actions (5) and (7) the sum over k in (5) has to be transformed to the energy integral

$$\sum_k V(\varepsilon_k)^2 G_{nm}^c(k) = \int_{-1}^1 d\varepsilon V(\varepsilon)^2 \rho(\varepsilon) G_{nm}^c(\varepsilon). \quad (8)$$

This also defines the density of states for the free conduction electrons $\rho(\varepsilon)$. The equivalence of the effective actions (5) and (7) leads to the condition

$$\int_{-1}^1 dg \frac{\partial \varepsilon(g)}{\partial g} h(\varepsilon(g))^2 G_{nm}^c(g) \equiv \int_{-1}^1 d\varepsilon V(\varepsilon)^2 \rho(\varepsilon) G_{nm}^c(\varepsilon). \quad (9)$$

This can only be fulfilled for

$$\frac{\partial \varepsilon(x)}{\partial x} h(\varepsilon(x))^2 = V(x)^2 \rho(x), \quad (10)$$

(with $\varepsilon(x)$ the inverse of $g(\varepsilon)$). For a given $\Delta(x) \equiv \pi V(x)^2 \rho(x)$ there are obviously many ways of dividing the energy dependence between $\varepsilon(x)$ and the dispersion $h(\varepsilon(x))$. One possibility is to choose

$$g(\varepsilon) = \varepsilon \quad \text{and} \quad h(\varepsilon)^2 = \frac{1}{\pi} \Delta(\varepsilon). \quad (11)$$

For $\Delta(\varepsilon) = \Delta$ eq. (11) corresponds to the standard case (see eq. (2.4) in [7]). It might also be convenient to set $h(\varepsilon) = h$. Together with the condition $\varepsilon(-1) = -1$ and $\varepsilon(1) = 1$ this leads to

$$\varepsilon(g) = -1 + \frac{1}{\pi h^2} \int_{-1}^g dx \Delta(x) \quad \text{and}$$

$$h^2 = \frac{1}{2\pi} \int_{-1}^1 d\varepsilon \Delta(\varepsilon). \quad (12)$$

This equations also reduce to $\varepsilon(g) = g$ and $h^2 = \frac{1}{\pi} \Delta$ for a constant $\Delta(\varepsilon) = \Delta$. Equations (11) and (12) have

already been derived by CY [13]. In a subsequent publication [8] these authors use eq. (12) for the mapping of the Kondo model on a semi-infinite chain (see Appendix A for a discussion of the resulting hopping matrix elements).

The first possibility eq. (11) has a conceptual disadvantage arising from the logarithmic discretization of the conduction band. Within each interval $[x_{n+1}, x_n]$ and $[-x_n, -x_{n+1}]$, with $x_n = \Lambda^{-n}$, the conduction electron operators are expressed in terms of a Fourier expansion. As long as $h(\varepsilon)^2$ is constant in each interval, the impurity couples only to the average component ($p=0$) of the conduction electrons. Therefore it is reasonable to neglect all the $p \neq 0$ -states (this becomes exact in the limit $\Lambda \rightarrow 1$). This line of reasoning obviously does not hold for eq. (11).

On the other hand, the energy dependence of $\Delta(\varepsilon)$ can be taken into account in the hybridization by defining $h(\varepsilon)^2$ as the mean value

$$h_n^{\pm 2} = \frac{1}{d_n} \int^{\pm} d\varepsilon \frac{1}{\pi} \Delta(\varepsilon), \quad (13)$$

$$\int^+ d\varepsilon \equiv \int_{x_{n+1}}^{x_n} d\varepsilon, \quad \int^- d\varepsilon \equiv \int_{-x_n}^{-x_{n+1}} d\varepsilon, \quad (14)$$

(with $d_n = x_n - x_{n+1}$) in each interval of the logarithmic discretization. This is so far not an approximation as the remaining energy dependence will be incorporated in the dispersion. The advantage of an energy dependent hybridization as in eq. (13) is that the resulting dispersion has the form $g(\pm x_n) = \pm x_n$ for all n , i.e. at all points x_n of the logarithmic discretization. This "linear" form (for intermediate values $g(\varepsilon) = \varepsilon$ is not fulfilled) leads to a scaling behaviour of the hopping matrix elements (see eq. (27)) of the form $t_n \propto \Lambda^{-n/2}$, slightly modified due to the structure of $\Delta(\varepsilon)$. The representation eq. (12), however, leads to a scaling with an effective Λ_{eff} not equal to Λ which might even depend on the number of iterations thus making the analyses (of the fixed points, the relevant energy scale, etc.) more difficult.

For these reasons, we take the representation eq. (13) in the following. This gives for the hybridization part of the discretized Hamiltonian

$$H_{\text{hyb}} = \sqrt{\frac{\xi_0}{\pi}} \left[f_{-1\sigma}^\dagger f_{0\sigma} + f_{0\sigma}^\dagger f_{-1\sigma} \right], \quad (15)$$

with

$$f_{0\sigma} = \frac{1}{\sqrt{\xi_0}} \sum_n \left[\gamma_n^+ a_{n\sigma} + \gamma_n^- b_{n\sigma} \right], \quad (16)$$

$$\xi_0 = \sum_n \left((\gamma_n^+)^2 + (\gamma_n^-)^2 \right) = \int_{-1}^1 d\varepsilon \Delta(\varepsilon), \quad (17)$$

$$(\gamma_n^\pm)^2 = \int^{\pm} d\varepsilon \Delta(\varepsilon). \quad (18)$$

The discrete conduction electron operators $a_{n\sigma}$ ($b_{n\sigma}$) for positive (negative) ε correspond to those introduced in [6,7]. According to the differential equation (10) we should now have to solve for $\varepsilon(x)$ and invert $\varepsilon(x)$ to obtain the dispersion $x(\varepsilon) \equiv g(\varepsilon)$. This is actually not necessary because the single-particle energies in the conduction electron part of the discretized Hamiltonian

$$H_c = \sum_{n\sigma} \left[\xi_n^+ a_{n\sigma}^\dagger a_{n\sigma} + \xi_n^- b_{n\sigma}^\dagger b_{n\sigma} \right] \quad (19)$$

only depend on the integral over $g(\varepsilon)$

$$\xi_n^\pm = \frac{1}{d_n} \int^{\pm} d\varepsilon g(\varepsilon). \quad (20)$$

It can be shown that the discrete energies ξ_n^\pm are given by

$$\xi_n^\pm = \frac{\int^{\pm} d\varepsilon \Delta(\varepsilon) \varepsilon}{\int^{\pm} d\varepsilon \Delta(\varepsilon)}. \quad (21)$$

This equation, together with the form of the hybridization part has already been used by Sakai et al. [14], although no derivation was given in their article.

The discretized Hamiltonian for the single-impurity Anderson model now takes the form

$$\begin{aligned} H = & \sum_{\sigma} \varepsilon_f f_{-1\sigma}^\dagger f_{-1\sigma} + U f_{-1\uparrow}^\dagger f_{-1\uparrow} f_{-1\downarrow}^\dagger f_{-1\downarrow} \\ & + \sum_{n\sigma} \left[\xi_n^+ a_{n\sigma}^\dagger a_{n\sigma} + \xi_n^- b_{n\sigma}^\dagger b_{n\sigma} \right] \\ & + \sqrt{\frac{\xi_0}{\pi}} \left[f_{-1\sigma}^\dagger f_{0\sigma} + f_{0\sigma}^\dagger f_{-1\sigma} \right]. \end{aligned} \quad (22)$$

III. PSEUDOGAP DENSITY OF STATES — MAPPING ON SEMI-INFINITE CHAIN

We now consider a $\Delta(\omega)$ of the form

$$\Delta(\omega) = \Delta_0 |\omega|^r, \quad -1 \leq \omega \leq 1. \quad (23)$$

The discrete energies ξ_n^\pm of the conduction electrons and the hybridization matrix elements γ_n^\pm between impurity and the conduction electrons take the form

$$\xi_n^+ = -\xi_n^- = \frac{r+1}{r+2} \frac{1 - \Lambda^{-(r+2)}}{1 - \Lambda^{-(r+1)}} \Lambda^{-n} \quad (24)$$

and

$$(\gamma_n^+)^2 = (\gamma_n^-)^2 = \frac{\Delta_0}{r+1} \Lambda^{-n(r+1)} \left(1 - \Lambda^{-(r+1)} \right). \quad (25)$$

The mapping of the discretized Hamiltonian (22) onto the semi-infinite chain form

$$H = \sum_{\sigma} \varepsilon_f f_{-1\sigma}^{\dagger} f_{-1\sigma} + U f_{-1\uparrow}^{\dagger} f_{-1\uparrow} f_{-1\downarrow}^{\dagger} f_{-1\downarrow} + \sum_{\sigma n=0}^{\infty} t_n \left[f_{n\sigma}^{\dagger} f_{n+1\sigma} + f_{n+1\sigma}^{\dagger} f_{n\sigma} \right] \quad (26)$$

$$+ \sqrt{\frac{\xi_0}{\pi}} \left[f_{-1\sigma}^{\dagger} f_{0\sigma} + f_{0\sigma}^{\dagger} f_{-1\sigma} \right], \quad (27)$$

($\xi_0 = \frac{2\Delta_0}{r+1}$) is described in [6] and [7]. The only difference appearing here is the r -dependence of the ξ_n^{\pm} and γ_n^{\pm} . (Note that in the non-symmetric case additional terms of the form $\varepsilon_n f_{n\sigma}^{\dagger} f_{n\sigma}$ are generated.) For the hopping matrix elements t_n we find the following expressions.

$$t_n = \Lambda^{-n/2} \frac{r+1}{r+2} \frac{1-\Lambda^{-(r+2)}}{1-\Lambda^{-(r+1)}} \left[1 - \Lambda^{-(n+r+1)} \right] \times \left[1 - \Lambda^{-(2n+r+1)} \right]^{-1/2} \left[1 - \Lambda^{-(2n+r+3)} \right]^{-1/2} \quad (28)$$

for even n and

$$t_n = \Lambda^{-(n+r)/2} \frac{r+1}{r+2} \frac{1-\Lambda^{-(r+2)}}{1-\Lambda^{-(r+1)}} \left[1 - \Lambda^{-(n+1)} \right] \times \left[1 - \Lambda^{-(2n+r+1)} \right]^{-1/2} \left[1 - \Lambda^{-(2n+r+3)} \right]^{-1/2} \quad (29)$$

for odd n . The equations (28) and (29) have been verified numerically and by analytical calculation of t_0 and t_1 . In the limit $n \rightarrow \infty$ (28) and (29) reduce to

$$t_n \xrightarrow{n \rightarrow \infty} \frac{r+1}{r+2} \frac{1-\Lambda^{-(r+2)}}{1-\Lambda^{-(r+1)}} \Lambda^{-n/2} \begin{cases} 1 & : n \text{ even} \\ \Lambda^{-r/2} & : n \text{ odd} \end{cases} \quad (30)$$

This limit of the hopping matrix elements has also been found by Ingersent [9] although the formula for *all* n is not given in his paper. The result obtained by CY is discussed in the appendix.

An analytical form of the t_n for all $n \geq 0$ can only be given when the powerlaw $\Delta(\omega) = \Delta_0 |\omega|^r$ extends to the band edges. In any experimental realization, however, we expect this powerlaw only to be valid near the Fermi level. On the other hand, numerical studies show that any deviation from the form (23) close to the band edges merely affects the first coefficients, while the asymptotic behaviour again depends on r only and is given by (30). Thus the qualitative behaviour near the possible low temperature fixed points is not affected by the exact form of $\Delta(\omega)$ away from the Fermi level.

IV. RESULTS FOR STATIC PROPERTIES

The Hamiltonian (26) is solved with the NRG for the parameters $\varepsilon_f = -U/2 = 10^{-3}$, $\Lambda = 2.5$ and different values for r and Δ_0 . At each iteration step we keep ≈ 500

states which is sufficient for the calculation of thermodynamic properties.

We first want to discuss the phase-diagram of Fig. 1 where we have plotted the critical value Δ_c versus r . For any $\Delta_0 > \Delta_c$ the system flows to a strong-coupling fixed point (SC) similar to the fixed point in the standard case [7]. The energy spectrum at this fixed point can be explained by removing the first conduction electron site from the chain due to its strong coupling to the impurity. The remaining chain, however, has a different structure as compared to the $r=0$ -case. Therefore this SC fixed point has not the Fermi liquid properties of the standard single-impurity Anderson model (see below). For $\Delta_0 < \Delta_c$ the system always flows to the local-moment fixed point (LM) with the impurity effectively decoupled from the conduction band. Again, the resulting energy levels are in agreement with those of the free conduction electron chain.

For both the Kondo model and the Anderson model $\Delta_c(r)$ diverges at $r = \frac{1}{2}$ and we find for the Anderson model a logarithmic divergence

$$\Delta_{c,A}(r) \propto -\ln\left(\frac{1}{2} - r\right). \quad (31)$$

However, the behaviour of $\Delta_c(r)$ for $0 < r < \frac{1}{2}$ is quite different for both models. Ingersent finds an extended linear region $\Delta_c(r) \propto r$ which is approximately valid up to values of $r = 0.4$ (see inset of Fig. 1). In our case, $\Delta_c(r)$ also starts linearly and is in agreement with the result for the Kondo model up to $r \approx 0.02$, but increases far more rapidly for larger r .

The difference to [9] is mainly due to the fact that for the parameters used here, the f -level lies within the pseudogap density of states. Under the assumption that the relevant coupling Δ' for this problem is (approximately) the value $\Delta(\omega = \varepsilon_f)$ we have the exponential dependence

$$\Delta'(r) \approx \Delta_0 |\varepsilon_f|^r = \Delta_0 e^{r \ln |\varepsilon_f|}. \quad (32)$$

As $\ln |\varepsilon_f|$ has a large negative value, $\Delta'(r)$ is strongly suppressed for increasing r so that a much larger Δ_0 is needed to reach the strong coupling fixed point. This increase of the parameter regime in which local moment formation is observed has also been found by Gonzalez-Buxton and Ingersent [15] who applied a poor man's scaling approach to the Anderson version of the pseudogap problem. To show that eq. (32) basically explains the difference between the Kondo model and the Anderson model, we have plotted in the inset of Fig. 1 both $\Delta_{c,K}(r)$ for the Kondo model and $\Delta'_{c,A}(r) = \Delta_{c,A}(r) \cdot \exp(-7.9 \cdot r)$. (the value 7.9 was chosen in order to fit $\Delta'_{c,A}(r)$ to $\Delta_{c,K}(r)$) The linear region of $\Delta'_{c,A}(r)$ now extends to $r \approx 0.4$.

The remaining difference between $\Delta_{c,K}(r)$ and $\Delta_{c,A}(r)$ is due to the fact that the Kondo model and the Anderson model are related via the Schrieffer-Wolff transformation [10] only in the limit $J \rightarrow 0$ (corresponding to

$V^2/U \rightarrow 0$). Therefore, the agreement of the results for both models is only guaranteed for $\Delta \rightarrow 0$. Away from the line $\Delta = 0$, there is no exact mapping between the Kondo version and the Anderson version.

The critical coupling $\Delta_c(r)$ is determined as follows. Fig. 2 shows the temperature dependence of the effective magnetic moment for $U = 0.001$, $\varepsilon_f = -U/2$, $r = 0.48$ and different values of Δ . In this graph, the LM fixed point (characterized by $\mu_{\text{res}} \equiv \mu_{\text{eff}}(T \rightarrow 0) = 1/4$) is reached within the given temperature range for $\Delta = 0.01$ and $\Delta = 0.02$. The value $\mu_{\text{res}} = r/8 = 0.06$ corresponding to the SC fixed point is clearly approached for $\Delta = 0.16$ while for $\Delta = 0.04$ this value should be reached at a much lower temperature. From Fig. 2 we determine $\Delta_c(r = 0.48)$ as ≈ 0.03 and repeat this procedure for different values of r . Similar results for $\mu_{\text{eff}}(T)$ have been obtained by Ingersent and CY.

The value $\mu_{\text{res}} = r/8$ at the SC fixed point can also be derived directly from the semi-infinite chain form of the free conduction electron chain at this fixed point. One simply has to compare the effective magnetic moment for the system with and without the first conduction electron site.

The temperature dependence of the specific heat coefficient $\gamma(T) = C(T)/T$ in the SC regime is shown in Fig. 3. The low temperature behaviour of $\gamma(T)$ is described by a power law of the form

$$\gamma(T) = c_1 T^{-r} + c_2 T^{-2r}. \quad (33)$$

Although eq. (33) resembles an expansion in T^{-r} , there cannot be any terms like T^{-3r} , T^{-4r} etc. as the corresponding entropy would then diverge for $T \rightarrow 0$ (for e.g. $r = 0.4$).

The exponent α defined by $\gamma(T) \propto T^\alpha$ is shown in the inset of Fig. 3. In an intermediate temperature regime, α approaches the value $-r$ consistent with the result of CY. However, for lower temperatures another term with the exponent $\alpha = -2r$ is dominating. This term is strongly suppressed in the intermediate regime due to $c_2 \ll c_1$. This crossover from the T^{-r} to the T^{-2r} behaviour is *not* due to a crossover to a new low temperature fixed point. For the spin susceptibility we confirm the result given by CY:

$$\chi(T) = \frac{r}{8} T^{-1} + c'_1 T^{-r} + c'_2 T^{-2r}. \quad (34)$$

In the LM regime we find

$$\gamma(T) = c_3 T^{r-1}. \quad (35)$$

and

$$\chi(T) = \frac{1}{4} T^{-1} + c'_3 T^{r-1}. \quad (36)$$

V. RESULTS FOR THE SPECTRAL FUNCTION

The impurity spectral function

$$A(\omega) = \frac{1}{Z} \sum_{nm} \left| \langle n | f_{-1\sigma}^\dagger | m \rangle \right|^2 \delta(\omega - (E_n - E_m)) \times (e^{-\beta E_m} + e^{-\beta E_n}), \quad (37)$$

(with the partition function $Z = \sum_m \exp(-\beta E_m)$), has not yet been calculated in the previous papers on the pseudogap problem. We assume that the groundstate energy E_g is set to zero and concentrate on the zero-temperature limit, in which the spectral function takes the form

$$A(\omega) = \frac{1}{Z} \left\{ 2 \sum_{n_g m_g} \left| \langle n_g | f_{-1\sigma}^\dagger | m_g \rangle \right|^2 \delta(\omega) + \sum_{n_g m_e} \left| \langle n_g | f_{-1\sigma}^\dagger | m_e \rangle \right|^2 \delta(\omega + E_{m_e}) + \sum_{n_e m_g} \left| \langle n_e | f_{-1\sigma}^\dagger | m_g \rangle \right|^2 \delta(\omega - E_{n_e}) \right\}. \quad (38)$$

Here, the partition function Z equals the total degeneracy of the groundstate. The n_g, m_g label all states with energy $E = E_g = 0$ and the n_e, m_e label the excited states. The first term in eq. (38) would correspond to a transition between different states with $E = 0$, but such a term (resulting in a δ -function at the Fermi level) is not present in the NRG results. There is one state with excitation energy $E_{\text{ex}} \rightarrow 0$ for $N \rightarrow \infty$ but its matrix element with the ground state vanishes as $N \rightarrow \infty$.

In order to obtain the full frequency dependence of the spectral function within the NRG, it is necessary to combine the information of all iteration steps as in each iteration the results are only given for a certain frequency range (see also [16,17]).

In Fig. 4 we show results for the spectral function for $r = 0.25$, $\Delta > \Delta_c$ (solid line, SC regime), $r = 0.25$, $\Delta < \Delta_c$ (dotted line, LM regime) and $r = 0.75$ (dashed line, LM regime). For these calculations we used $\Lambda = 2$ and kept ≈ 800 states at each iteration.

We find that $A(\omega)$ diverges as $|\omega|^{-r}$ for $\omega \rightarrow 0$ for any set of parameters which lies in the SC regime. Note that this result suggests the conventional behaviour $A(\omega) \sim 1/(\pi\Delta(\omega))$ as $\omega \rightarrow 0$ for the SC case. Together with the result $\gamma(T) \sim T^{-r}$ (neglecting the second term in (33) for the moment) one could be tempted to interpret these results within a standard Fermi liquid approach. Let us however emphasize that in spite of these results the system is not a Fermi liquid for any $r > 0$.

This observation becomes more evident in the LM regime, where the behaviour of the spectral function is qualitatively different. Namely, in contrast to the SC case we find that the spectral function vanishes as $A(\omega) \propto |\omega|^r$

here. In addition, no qualitative difference, apart from the exponent, can be observed between the cases $r > 0.5$ and $r < 0.5$.

VI. SUMMARY

To summarize, we have studied the problem of an Anderson impurity in a pseudo-gap Fermi system at particle-hole symmetry using a generalization of the numerical renormalization group method [6,7]. We find a behaviour similar to that of the corresponding Kondo model investigated by CY [8] and Ingersent [9]. However, the critical line Δ_c separating the strong-coupling and local-moment regimes of these two models shows a quite different form between $r=0$ (where Δ_c starts linearly) and $r=1/2$ (where Δ_c diverges). This difference is mainly due to the fact that we have chosen the f-level to lie within the pseudogap. In both strong-coupling and local-moment regime the thermodynamic quantities specific heat and spin-susceptibility show powerlaw behaviour.

We also presented the first calculations of the impurity spectral function for this model. We find $A(\omega) \propto |\omega|^{-r}$ in the strong-coupling regime and $A(\omega) \propto |\omega|^r$ in the local-moment regime. We do not find any indication that the local moment fixed points for $r < 1/2$ and $r > 1/2$ are different.

As shown by Ingersent for the Kondo model, the critical values Δ_c take finite values as soon as particle-hole symmetry is violated. It is of course interesting to see, whether this reduction of the critical coupling is the same for the Anderson model (work on this problem is in progress).

Another interesting question is the relevance of the model studied here in the context of the dynamical mean field theory (for recent reviews see [18,19]). The effective single impurity Anderson model appearing in the dynamical mean field theory is coupled to a (self-consistently determined) effective medium. There is a possibility that the density of states corresponding to this effective medium develops a pseudo-gap structure under certain conditions (e.g. near the metal-insulator transition). Also, the density of states of the infinite dimensional generalization of the honeycomb ($d=2$) and diamond ($d=3$) lattices is proportional to $|\omega|$ near the Fermi level.

We wish to thank J. Keller and G. M. Zhang for a number of stimulating discussions. One of us (R.B.) was supported by a grant from the Deutsche Forschungsgemeinschaft, grant No. Bu965-1/1.

APPENDIX A: OTHER DISCRETIZATION SCHEMES

In this appendix, we want to show that the discretization used by CY leads to the same hopping matrix elements t_n apart from a redefinition of the discretization parameter Λ . This equivalence, however, is restricted to the special form of $\Delta(\omega)$ and is not valid in general.

For $\Delta(\omega) = \Delta_0|\omega|^r$ eq. (12) leads to

$$g(\varepsilon) = \varepsilon^{\frac{1}{r+1}}, \quad (\text{A1})$$

$$h^2 = \frac{\Delta_0}{\pi} \frac{1}{r+1}. \quad (\text{A2})$$

The discrete energies ξ_n^\pm take the form

$$\begin{aligned} \xi_n^+ &= -\xi_n^- = \frac{1}{d_n} \int_0^+ d\varepsilon g(\varepsilon) \\ &= \frac{r+1}{r+2} \frac{1 - \Lambda^{-\frac{r+2}{r+1}}}{1 - \Lambda^{-1}} \Lambda^{-\frac{n}{r+1}} \\ &= \frac{r+1}{r+2} \frac{1 - \bar{\Lambda}^{-(r+2)}}{1 - \bar{\Lambda}^{-(r+1)}} \bar{\Lambda}^{-n}. \end{aligned} \quad (\text{A3})$$

In the last equation we have defined $\bar{\Lambda} = \Lambda^{\frac{1}{r+1}}$.

The hybridization in eq. (A2) is independent of frequency, therefore the result for $(\gamma_n^\pm)^2$ is the same as for a constant $\Delta(\omega) = \Delta_0/(r+1)$

$$(\gamma_n^\pm)^2 = \frac{\Delta_0}{r+1} \Lambda^{-n} (1 - \Lambda^{-1}). \quad (\text{A4})$$

With $\Lambda = \bar{\Lambda}^{(r+1)}$ eq. (A4) gives

$$(\gamma_n^\pm)^2 = \frac{\Delta_0}{r+1} \bar{\Lambda}^{-n(r+1)} (1 - \bar{\Lambda}^{-(r+1)}). \quad (\text{A5})$$

Eqs. (A3) and (A5) correspond to Eqs. (24) and (25) with Λ being replaced by $\bar{\Lambda}$. Obviously, also the resulting matrix elements t_n will have exactly the same form as in eqs. (28) and (29) and in terms of Λ we find in the limit of large N

$$t_n \xrightarrow{n \rightarrow \infty} \frac{r+1}{r+2} \frac{1 - \Lambda^{-\frac{r+2}{r+1}}}{1 - \Lambda^{-1}} \Lambda^{-\frac{n}{2(r+1)}} \begin{cases} 1 & : n \text{ even} \\ \Lambda^{-\frac{r}{2(r+1)}} & : n \text{ odd} \end{cases}. \quad (\text{A6})$$

For the ratio of t_n/t_{n-1} we then find

$$\frac{t_n}{t_{n-1}} \xrightarrow{n \rightarrow \infty} \begin{cases} \Lambda^{\frac{r-1}{2(r+1)}} & : n \text{ even} \\ \Lambda^{-1/2} & : n \text{ odd} \end{cases}, \quad (\text{A7})$$

corresponding to the result given in CY.

- [1] A. C. Hewson, *The Kondo Problem to Heavy Fermions* (Cambridge Univ. Press, Cambridge, 1993).
- [2] D. Withoff, E. Fradkin: Phys. Rev. Lett. **64**, 1835 (1990)
- [3] M. Sigrist, K. Ueda: Rev. Mod. Phys. **63**, 239 (1991)
- [4] B. A. Volkov, O. A. Pankratov: Pis'ma Zh. Eksp. Teor. Fiz. **42**, 145 (1985) [JETP Lett. **42**, 178 (1985)]
- [5] B. Dardel, D. Malterre, M. Grioni, P. Weibel, Y. Baer, J. Voit and D. Jérôme: Phys. Rev. Lett. **24**, 687 (1993)
- [6] K. G. Wilson: Rev. Mod. Phys. **47**, 773 (1975)
- [7] H. R. Krishna-murthy, J. W. Wilkins and K. G. Wilson: Phys. Rev. **B21**, 1003 & 1044 (1980)
- [8] K. Chen, C. Jayaprakash: J. Phys.: Cond. Matter **7**, L491 (1995)
- [9] K. Ingersent: Phys. Rev. B **54**, 11936 (1996)
- [10] J. R. Schrieffer, P. A. Wolff: Phys. Rev. **159**, 491 (1966)
- [11] The restriction to a hybridization depending on k only through ε_k is not necessary but convenient for pedagogical reasons.
- [12] R. Bulla, J. Keller and T. Pruschke: Z. Phys. B **94**, 195 (1994)
- [13] Kan Chen, C. Jayaprakash: Phys. Rev. B **52**, 14436 (1995)
- [14] O. Sakai, Y. Kuramoto: Sol. Stat. Comm. **89**, 307 (1994)
- [15] C. Gonzalez-Buxton and K. Ingersent: Phys. Rev. B **54**, 15614 (1996)
- [16] T. A. Costi, A. C. Hewson, V. Zlatic: J. Phys.: Cond. Matter **6**, 2519 (1994)
- [17] O. Sakai, Y. Shimizu, T. Kasuya: J. Phys. Soc. Jpn. **58**, 3666 (1989)
- [18] T. Pruschke, M. Jarrell and J. K. Freericks: Adv. Phys. **44**, 187 (1995)
- [19] A. Georges, G. Kotliar, W. Krauth and M. J. Rozenberg: Rev. Mod. Phys. **68**, 13 (1996)
- [20] G. Santoro, M. Airoidi, S. Sorella and E. Tosatti: Phys. Rev. B **47**, 16216 (1993)

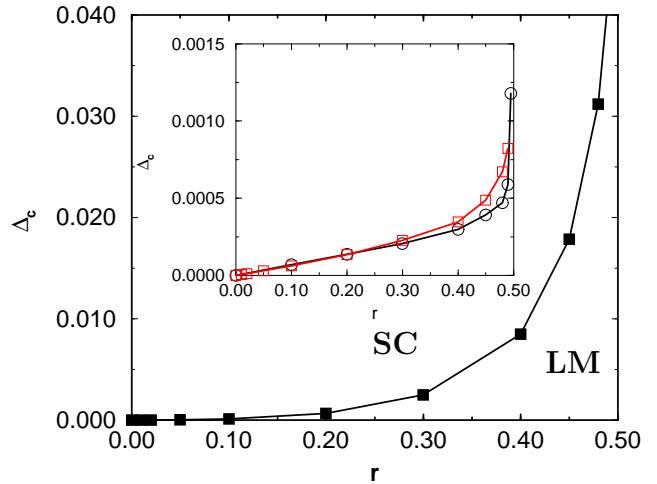


FIG. 1. r -dependence of the critical coupling Δ_c which separates the strong-coupling regime ($\Delta > \Delta_c$) from the local-moment regime ($\Delta < \Delta_c$). The filled squares show the result for $\Delta_{c,A}(r)$. In the inset we compare the scaled critical coupling $\Delta'_{c,A}(r)$ (open squares) with the result obtained by Ingersent for the Kondo version of the Hamiltonian (3) (circles).

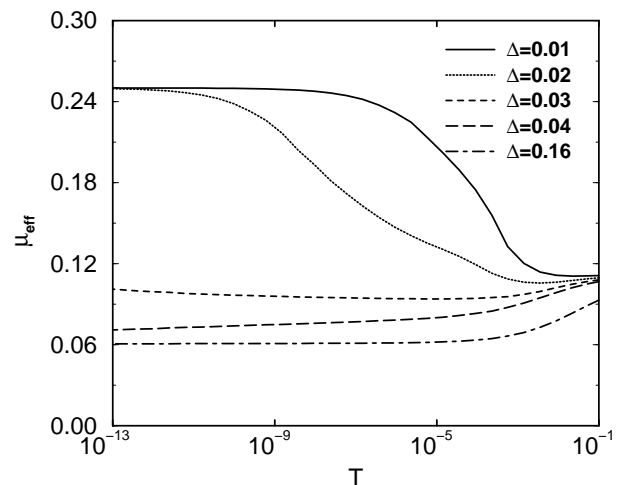


FIG. 2. Temperature dependence of the effective magnetic moment for $U = 0.001$, $\varepsilon_f = -U/2$, $r = 0.48$ and various values of Δ . For $\Delta < 0.03$, the system flows to the local-moment fixed point with the corresponding effective magnetic moment $\mu_0 = 1/4$. For $\Delta > 0.03$ the magnetic moment is partially screened and approaches the residual value $\mu_{res} = r/8 = 0.06$ from above.

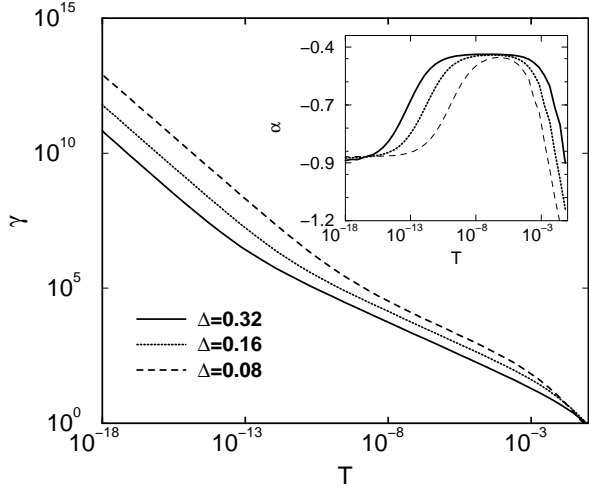


FIG. 3. Temperature dependence of the specific heat coefficient $\gamma(T) = C(T)/T$ for $U = 0.001$, $\varepsilon_f = -U/2$, $r = 0.48$ and various values of Δ . The inset shows the temperature dependence of the exponent $\alpha(T)$ defined by $\gamma(T) \propto T^\alpha$. In an intermediate regime, α approaches $-r$ as expected from eq. (1) but for lower temperatures a stronger divergent term with $\alpha \approx -0.93 \approx -2r$ dominates. This behaviour is not due to the crossover to a new fixed point.

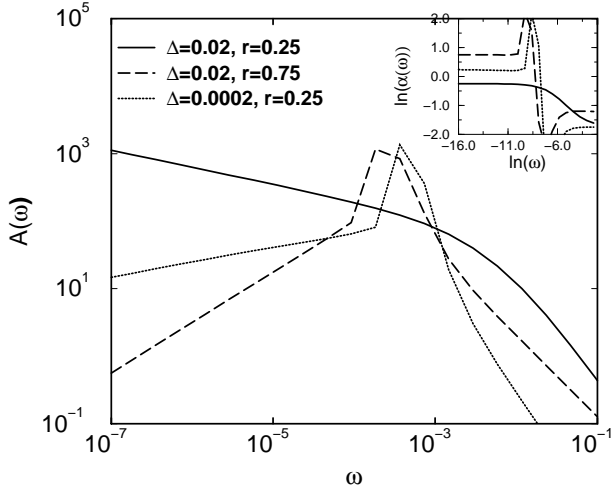


FIG. 4. Impurity spectral function for $U = 0.001$, $\varepsilon_f = -U/2$, and different values of r and Δ . for $r = 0.25$ and $\Delta = 0.02$ (solid line, SC-regime), the spectral function diverges as $A(\omega) \propto |\omega|^{-r}$ for $|\omega| \rightarrow 0$. In the LM-regime (for both $r = 0.25$ and $\Delta = 0.0002$ (dotted line) and $r = 0.75$ and $\Delta = 0.02$ (dashed line)) the spectral function vanishes as $|\omega|^r$. The inset shows the coefficient $\alpha(\omega)$ defined by $A(\omega) \propto |\omega|^{\alpha(\omega)}$.